ACS ENGINEERING Au
AN OPEN ACCESS JOURNAL OF THE AMERICAN CHEMICAL SOCIETY



pubs.acs.org/engineeringau
Article

# Competing Effects of Molecular Additives and Cross-Link Density on the Segmental Dynamics and Mechanical Properties of Cross-Linked Polymers

*Published as part of the ACS Engineering Au virtual special issue "Materials Design".*

Wenjian Nie, Jack F. Douglas,* and Wenjie Xia*

Cite This: *ACS Eng. Au* 2023, 3, 512–526
Read Online



**ABSTRACT:** The introduction of molecular additives into thermosets often results in changes in their dynamics and mechanical properties that can have significant ramifications for diverse applications of this broad class of materials such as coatings, high-performance composites, *etc.* Currently, there is limited fundamental understanding of how such additives influence glass formation in these materials, a problem of broader significance in glass-forming materials. To address this fundamental problem, here, we employ a simplified coarse-grained (CG) model of a polymer network as a model of thermoset materials and then introduce a polymer additive having the same inherent rigidity and polymer−polymer interaction strength as the cross-linked polymer matrix. This energetically "neutral" or "self-plasticizing" additive model gives rise to non-trivial changes in the dynamics of glass formation and provides an important theoretical reference point for the technologically more important case of interacting additives. Based on this rather idealized model, we systematically explore the combined effect of varying the additive mass percentage ($m$) and cross-link density ($c$) on the segmental relaxation dynamics and mechanical properties of a model thermoset material with additives. We find that increasing the additive mass percentage $m$ progressively decreases both the glass-transition temperature $T_g$ and the fragility of glass formation, a trend *opposite* to increasing $c$ so that these thermoset variables clearly have a *competing effect* on glass formation in these model materials. Moreover, basic mechanical properties (*i.e.*, bulk, shear, and tensile moduli) likewise exhibit a competitive variation with the increase of $m$ and $c$, which are strongly correlated with the Debye−Waller parameter $\langle u^2 \rangle$, a measure of material stiffness at a molecular scale. Our findings prove beneficial in the development of structure−property relationships for the cross-linked polymers, which could help guide the design of such network materials with tailored physical properties.

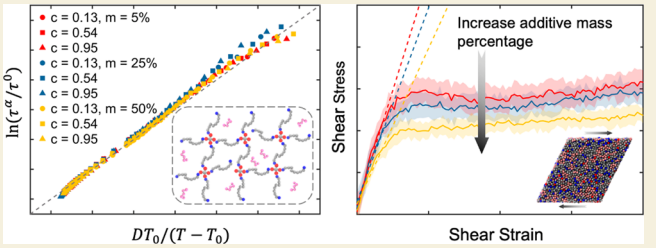


**KEYWORDS:** *cross-linked polymers, thermosets, molecular additives, glass formation, segmental relaxation, molecular dynamics simulations, fragility*

## 1. INTRODUCTION

Cross-linked thermosetting polymers are widely used in various engineering and technological applications owing to their excellent mechanical properties, thermal stability, and chemical resistance.[1,2] As polymer melts approach their glass transition temperatures ($T_g$), they experience a "solidification" process that is marked by a rapid drop in their relaxation dynamics and chain mobility, accompanied by an increase in stiffness. This behavior is commonly observed in glass-forming (GF) liquids, and this phenomenon can be observed through the processes of fast cooling,[3] sufficient pressurization,[3] or the curing of the thermoset through cross-linking at a fixed temperature ($T$),[4,5] a process referred to as "chemical vitrification". Despite the general ubiquity of glass formation in condensed materials, many aspects of this process remain insufficiently understood in terms of the fundamental origin of this transition or even the practical correlative understanding of the influences of the molecular structure and thermodynamic conditions on relaxation and diffusion and the mechanical properties of condensed materials. This is evidently a serious practical problem impeding the rational design of materials that have the properties required for material applications.

Considerable efforts have been made in simulating polymer GF materials with the aim of better comprehending how fundamental molecular parameters and thermodynamic

Received: August 15, 2023
Revised: September 30, 2023
Accepted: October 6, 2023
Published: November 9, 2023

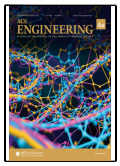

conditions [*e.g.*, additives,[6,7] molecular chemistry,[8,9] cross-link density,[10,11] cohesive energy,[12] chain stiffness,[13] polymer topology (*e.g.*, star, linear, branched, or cyclic architectures, and polymers with side groups),[14−18] and applied pressure[19,20]] influence thermodynamic and mechanical properties and relaxation in GF materials, such as $T_g$,[21,22] relaxation time,[20,23] dynamical heterogeneity,[11,24,25] and mechanical properties.[26,27] Due to the great importance of thermosetting materials in engineering and structural applications, in particular, exhaustive experiments have been performed to investigate the segmental relaxation dynamics of cross-linked thermosetting materials.[4,5,11,28−32] In particular, experimental studies based on model poly(methyl methacrylate) and polyvinyl ethylene have indicated that increasing the cross-link density of the network resulted in an increase in $T_g$ and fragility of glass formation that quantifies the strength of the temperature dependence of the relaxation time below the Arrhenius temperature $T_A$, along with the temperature range over which the glass transition takes place.[28,32] Apart from cross-link density, it has been shown that the chemical composition and monomer characteristics of GF polymers have a significant impact on influencing the fragility and relaxation dynamics. Specifically, it has been observed that polymers with greater packing frustration and rigidity tend to exhibit higher fragility of glass formation.[20,23,33] Some general trends of the physics of glass formation have been established based on significant collective scientific effort.

It has been observed that the incorporation of polar additives and nanoparticles (NPs) into thermoset polymers as well as the use of highly polar cross-linkers can lead to noteworthy alterations in the thermomechanical properties. For example, Reza *et al.*[34] employed SiC NPs coated with octaisobutyl polyhedral oligomeric silsesquioxane (OI-POSS) via a sonochemical process to establish a compatible interface between the particles and a thermoset polymer. Transmission electron microscopy (TEM) analysis of the OI-POSS-coated SiC NPs revealed enhanced attachment between the two particles. Incorporation of SiC and OI-POSS-coated SiC into the epoxy system resulted in improved flexural strength, shear modulus, and $T_g$, compared to the neat epoxy resin.[35] One of the important and rather general influences of adding polar or hydrogen-bonding additives as a cross-linking agent or charged or polar molecular species[36] to a polymer material is the increase of the cohesive density energy of the material. Xia and co-workers[37] have recently shown that increasing the strength of the cohesive interaction can lead to a significant increase in $T_g$ while at the same time leading to a significant decrease in the fragility of glass formation in the thermoset material. This competing effect has been observed recently in polymer network materials with cross-links intended to model charged physical cross-links found in mussels.[38] These results collectively reveal another apparently general behavior of GF materials, changes in $T_g$ and fragility are related to factors altering the cohesive interaction strength of the material.

The recent work exploring the influence of cohesive interaction strength on glass formation indicates that computational research based on coarse-grained (CG) polymer models provides an excellent opportunity for the further exploration of structure−property relationships in thermoset polymer materials, and this naturally brings us to a computational investigation of the role of molecular additives in the properties of thermoset materials since such additives are normally encountered in applications of these materials.

Previous simulation studies have indicated that the segmental dynamics and mechanical properties of thermoset polymers can be significantly altered through the incorporation of diverse additives that modify intermolecular interactions within thermosetting polymers.[6,7,39,40] For example, Riggleman *et al.*[39] explored the effect of antiplasticizer molecular additives on the efficiency of molecular packing and elastic properties for a CG GF polymer melt, where the introduction of antiplasticizer additives was found to lead to an increase in the packing efficiency and increased bulk and shear moduli of the polymer material in the glassy state. Starr and Douglas[40] studied the impact of NPs on the fragility and cooperative string-like motion in a model GF polymer melt by CG molecular dynamics (MD) simulation, where the significant changes in both the fragility and the average length of string-like motion depended on the NP−polymer interaction and NP concentration. Stukalin *et al.*[41] systematically explored the plasticization and antiplasticization of polymer melts from a theoretical standpoint by altering the cohesive energy of the diluents utilizing the generalized entropy theory (GET) of the dynamics of GF polymer fluids. These analytical computations indicated that a plasticization effect occurred when small additives with weakly attractive interactions were introduced into the polymer matrix, while antiplasticization was observed for additives that were relatively small to the polymer segments and had a relatively strong attractive cohesive interaction with the polymer matrix in comparison to the polymer−polymer interaction strength. The GET calculations were thus broadly in accord with the simulations of Riggleman *et al.*[39]

Mangalara and Simmons[42] later employed MD simulations to show that oligomeric diluents could cause substantial changes in a polymer's $T_g$ and fragility, changes that reflected changes in the diluent chemical bulkiness, degree of polymerization, and molecular stiffness. They also found that the relaxation time of polymer was linked to variations in the high-frequency glassy modulus and Debye−Waller parameter $\langle u^2 \rangle$ and its relation to relaxation through the localization model of glass formation. As a natural continuation of these former computational studies aimed at glass formation in thermoset materials, we investigate the influence of additives with regard to the dynamics and mechanical responses of a CG model over a wide range of $T$, additive mass percentage, and cross-link density to better understand how these molecular parameters influence basic trends in glass formation in this class of materials.

In our previous studies, we have systematically investigated how the cross-link density and cohesive energy influence the segmental dynamics and the mechanical and thermodynamic properties of the same model thermoset material examined in this current study, but where there was no molecular additive.[37,43] Comparison to these observations allows us to assess the effect of additives on the dynamic and mechanical properties of cross-linked thermosets. The main purpose of these previous works[43] was to achieve a better understanding of the influence of the primary molecular factors determining the glass formation in network polymers, such as cross-link density,[43] cohesive energy strength,[37] and chain stiffness, on segmental dynamics and mechanical properties. In the present work, we extend this systemic study of molecular parameters on glass formation in thermosets to include a molecular additive. Our restriction to a molecular additive in the form of relatively short polymer chains having an identical polymer−polymer interaction as that between the polymer network


https://doi.org/10.1021/acsengineeringau.3c00043
ACS Eng. Au 2023, 3, 512−526

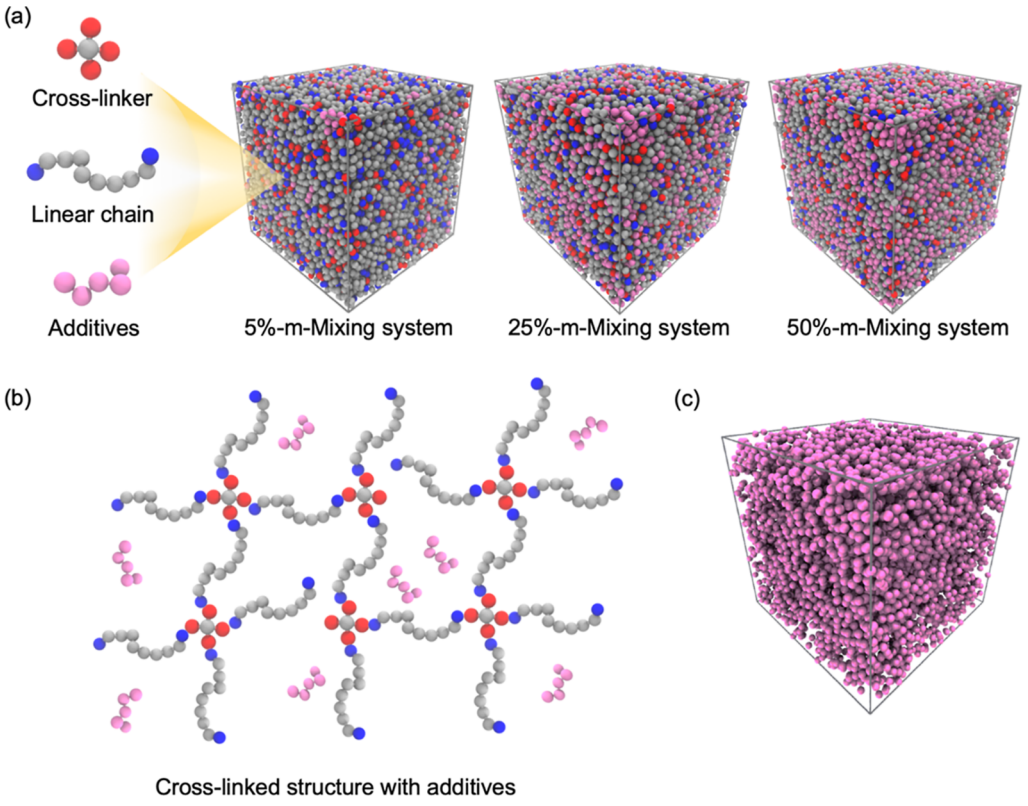


**Figure 1.** (a) Molecular structures of the cross-linker, linear chain, and additives, and snapshots of the cross-linked system with $m$ = 5, 25, and 50%, respectively. (b) Illustration of the cross-linked structure: red and blue beads represent reactive sites capable of undergoing cross-linking reactions in the cross-linker and linear chain, respectively. Specifically, each red bead can react with only one blue bead, and each cross-linker can link with a maximum of four linear chains. (c) Snapshot of dispersed additives within the matrix for $m$ = 25%.

segments is made in our initial study since changing this interaction would inevitably change the cohesive interaction strength of the material. We have avoided altering the molecular rigidity since molecular rigidity is also a significant factor altering the properties of GF liquids.[13,42,44] Finally, altering the polymer mass is known to alter the density of polymer materials, so we restrict our additives to have a *fixed molecular mass.* Despite these strong restrictions on the nature of the molecular additives, we find that increasing the additive concentration significantly alters the mechanical properties and segmental relaxation dynamics of the thermoset material. We note that our study of a neutral small additive can be achieved in practice by simply diluting the GF polymer material by the monomer or an oligomeric form of the high mass polymer material. There is a long history of studying this type of "blend" in relation to trying to understand shifts of the glass transition with molecular additives and in connection with understanding alterations of $T_g$ with changes in molecular mass.[45,46] Recent observations have shown that the addition of this type of self-plasticizing additive can greatly decrease the fragility of glass-formation which only a modest decrease of the glass transition. By way of the GET model discussed above, which really explains our simulation observations, at least qualitatively, we contrast the predictions of this type of "entropy theory" with the Gibbs and Dimarzio theory[47] which posits that glass formation corresponds to a second order phase transition at which the configuration entropy vanishes. Although this model does not describe the dynamics of glass formation, this model makes non-trivial prediction of the change of glass transition with molecular additives. Below, we observe a similar propensity of our "neutral" oligomer molecular additive to reduce the fragility of glass formation in our polymer model.

In future work, we plan to systematically explore the influence of the molecular rigidity of the additive and the strength of the intermolecular interaction of the additive molecules with each other in comparison to the interaction strength between the network segments and also the strength of the interaction between the network segments and the additive molecules (This effect was recently explored when the additive was taken to be a functionalized segment of the polymer[49]). All these molecular parameters are predicted by the GET to be important in understanding glass formation in polymer materials with additives.[41] Evidently, the parameter space governing the properties of these materials is rather large, and we must add additional relevant molecular variables to this parameter space. The present study is just one in a series aimed at understanding the most important molecular parameters of greatest importance for understanding and rationally engineering these complex materials, which is a suitable purpose for CG modeling.

## 2. MODEL AND SIMULATION DETAILS

### 2.1. Coarse-Grained Model

As shown in Figure 1a, the bead−spring CG cross-linked polymer model[48] utilized in this study consists of 1200 linear chains (each chain consists of 10 beads), 600 tetra-function star cross-linkers (each cross-linker consists of 5 beads), and the corresponding quantity of additives with different additive mass percentage (each additive consists of 5 beads) to discern


https://doi.org/10.1021/acsengineeringau.3c00043
ACS Eng. Au 2023, 3, 512−526

the impact of smaller chain additives, in comparison to the network chain length, on the network's properties. It is evident that additive sizes can induce more pronounced changes due to spatial network constraints, which will be addressed in forthcoming research. The additive mass percentage $m$ is defined as the mass of the additive divided by the total mass of the entire system. The systems with m of 5%, 25%, and 50% have 790, 5000, and 15,000 additive beads, respectively. In this work, we vary the additive mass percentage by fixing the number of networks and varying only the amount of the additives. The molecular structure used in this study incorporates additives with diverse mass percentages based on the model established in our previous research studies.[37,43] Periodic boundary conditions along all axes of the simulation cells are used to create representative bulk systems. The topology schematic of the polymer network structure with additives is illustrated in Figure 1b. To provide a clearer visual representation of the additives, Figure 1c shows a snapshot of the additives (from the 25% additive mass percentage system) within the simulation box, where the spatial distribution of the additives in the system can be observed.

The nonbonded interactions are described using the conventional truncated and shifted Lennard-Jones (LJ) potential,

$$U_{\mathrm{LJ}}(r) = \begin{cases} 4\varepsilon\left[\left(\frac{\sigma}{r}\right)^{12} - \left(\frac{\sigma}{r}\right)^{6} - \left(\frac{\sigma}{r_c}\right)^{12} + \left(\frac{\sigma}{r_c}\right)^{6}\right], & r < r_c \\ 0, & r \geq r_c \end{cases} \tag{1}$$

where $r$ is the beads distance, $r_c = 2.5\ \sigma$ is the cutoff distance, $\sigma$ dictates the effective van der Waals radius and signifies the distance at which the Lennard-Jones potential is zero, and $\varepsilon$ characterizes the depth of the potential well-connected to the strength of cohesive interactions. In this work, we assigned uniform values of $\sigma = 1$ and $\varepsilon = 1$ for all pairs within the system. This choice ensures that the interaction parameters remain consistent and allows for a standardized assessment of the system's behavior. The bonds between adjacent beads are modeled using the finitely extensible nonlinear elastic (FENE) potential,

$$U_{\mathrm{FENE}} = -0.5KR_0^2\ln\left[1 - \left(\frac{r}{R_0}\right)^2\right] + 4\varepsilon\left[\left(\frac{\sigma}{r}\right)^{12} - \left(\frac{\sigma}{r}\right)^{6}\right] + \varepsilon \tag{2}$$

where $K = 30\ \varepsilon/\sigma^2$ and $R_0 = 1.5\ \sigma$. The first term is characterized by attraction, while the second LJ term is marked by repulsion, featuring a reduced cutoff distance of $R_c = 2^{1/6}\sigma$. The restriction on bending is simulated through a straightforward cosine angular potential,

$$U_{\mathrm{bend}}(\theta) = k_\theta[1 + \cos(\theta)] \tag{3}$$

where $k_\theta$ describes the rigidity associated with bending, and $\theta$ represents the angle formed by three consecutively bonded particles. To investigate the impact of the additive mass percentage and cross-link density on flexible chains, we set the chain stiffness parameter $k_\theta$ of all chains as 0.2 $\varepsilon$. To simplify the calculations, all calculation quantities are expressed in reduced LJ units, with the length ($\sigma$), energy ($\varepsilon$), and mass ($m_0$) of each bead normalized to unity. A range of derived units can be derived from these basic units: *e.g.*, the temperature can be $T = \varepsilon/k_B$, and time in the unit of $\tau = (m_0\sigma^2/\varepsilon)^{1/2}$.

### 2.2. Simulation Details

All CG-MD simulations are conducted using the Large Scale Atomic/Molecular Massively Parallel Simulator (LAMMPS) software.[49] The initial mixture of different components undergoes equilibration and relaxation in an isobaric−isothermal ensemble (*NPT*) at a temperature of $T = 1.0$ and zero pressure, where a well-dispersed mixture system is achieved. Then, an iterative algorithm involving multiple cross-linking and relaxation steps developed by Varshney *et al.*[50] is utilized to interconnect the linear chains and cross-linkers to form three-dimensional networks, effectively capturing the thermodynamical and mechanical properties of cross-linked thermosets.[37,43,50,51] In each iteration, when the distance of the unreacted reactive bead pairs (a blue bead in the linear chain and a red bead in the cross-linker in Figure 1b) is less than the cutoff distance, a new bond is formed between the two reactive beads. Subsequently, an energy minimization procedure and an *NPT* relaxation process are carried out to reduce the energy fluctuations resulting from the introduction of new chemical bonds. When the reaction ratio of reactive beads exceeds 98% or there are no new bonds created, the cross-linking and relaxation cycle algorithm stops. The computational time for each iteration is 400 $\tau$. The schematic of the cross-linked network is shown in Figure 1b, where the chemical bonds formed between the blue and red beads signify that these reactive sites have undergone a reaction. Conversely, blue beads that are not linked to red beads indicate that the linear chains have not yet reacted with the cross-linker. The ratio of the total number of cross-links formed to the maximum number of cross-links that can be formed is defined as the cross-link density (*i.e.*, conversion rate) in this work.[52,53]

To explore how the relaxation dynamics and mechanical properties of cross-linked thermosets are affected by the cross-link density and additive mass percentage, we build nine systems with varying combinations of these parameters. First, these systems undergo equilibration in the *NPT* ensemble at a temperature of $T = 1.6$ for a duration of $t = 4 \times 10^4$ and then relaxation with the *NVT* ensemble takes $t = 2 \times 10^4$. Following this, a stepwise quenching process is applied from $T = 1.6$ to $T = 0.1$ with an incremental temperature step size of $\Delta T = 0.1$. At each temperature, the system is allowed to relax for $t = 2 \times 10^4$. Configurations are recorded at the end of each run, and the thermodynamic properties are averaged over a time interval of $t = 8 \times 10^3$. The systems with different cross-link densities ($c$) and additive mass percentages ($m$) are systematically simulated for investigations.

## 3. RESULTS AND DISCUSSION

### 3.1. Thermodynamic Properties

To examine the impact of the cross-link density and additive mass percentage on the thermodynamic properties of cross-linked thermosets, we estimate three fundamental quantities that characterize the thermodynamics of these materials, including the number density ($\rho$), thermal expansion coefficient ($\alpha_p$), and isothermal compressibility ($\kappa_T$). The results of thermodynamic properties as a function of $T$ are summarized in Figure S1 in the Supporting Information. As expected, the increase of $c$ and decrease of $m$ lead to a noticeable elevation in $\rho$, as well as a substantial reduction in $\alpha_p$ and $\kappa_T$ above $T_g$.[54,55] It should be noted that the influence


https://doi.org/10.1021/acsengineeringau.3c00043
ACS Eng. Au 2023, 3, 512−526

of the additive mass percentage parameter $m$ on the thermodynamic properties is comparable in order of magnitude as the effect of the cross-link density $c$.

Figure 2a shows the relationship between $\rho$ and $T$ for cross-linked systems with different values of $c$ and $m$. Across all

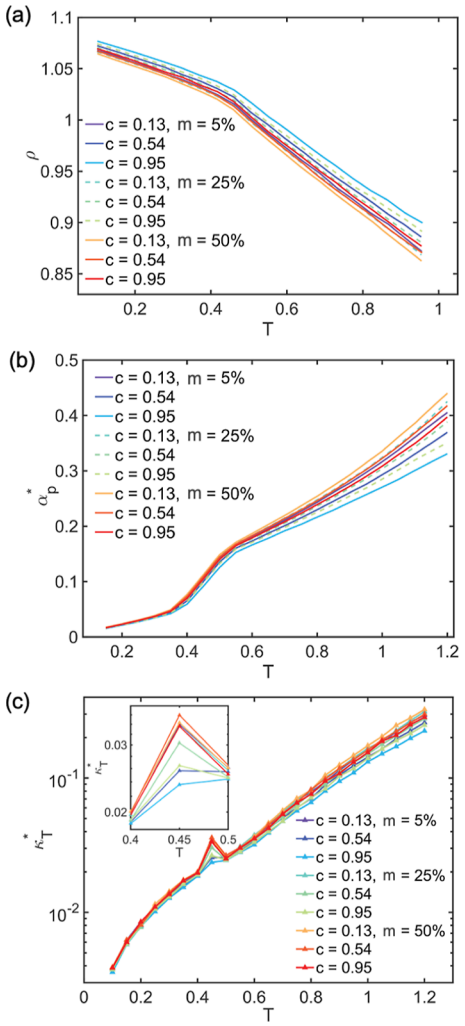


**Figure 2.** Different thermodynamic properties *vs* $T$ under different $c$ and $m$: (a) number density, $\rho$; (b) reduced thermal expansion coefficient, $\alpha_p^*$; and (c) reduced isothermal compressibility, $\kappa_T^*$. The inset shows a curious nonmonotonic behavior of $\kappa_T^*$.

systems, $\rho$ exhibits a nearly linear decline as $T$ rises at lower temperatures, followed by a more pronounced decrease above $T_g$. Furthermore, it is observed that $\rho$ increases with higher values of $c$ in systems with a constant $m$, a phenomenon extensively documented in cross-linked epoxy networks[54,55] and our previous cross-linked thermoset system without additives.[37,43] We also find that $\rho$ increases with the decrease of $m$ for systems with fixed $c$, mainly because the addition of additives makes the whole system expand; especially, a short chain length is chosen for the additives. The dimensionless properties $\alpha_p^*$ and $\kappa_T^*$ ($\alpha_p^* = T\alpha_p$ and $\kappa_T^* = \rho k_B T \kappa_T$), which are important properties in GET[13], are shown in Figure 2b,c. Both $\alpha_p^*$ and $\kappa_T^*$ increase obviously with elevating temperature above $T_g$, well consistent with that observed in the linear polymer melts and GET predictions.[13,19,56] Moreover, the higher $c$ system shows a smaller $\alpha_p^*$ and $\kappa_T^*$ because of the suppressed mobility of particles, which has been reported in our previous study on the cross-linked system without additives.[37,43] For systems with fixed $c$, the higher additives mass percentage leads to a larger $\alpha_p^*$ and $\kappa_T^*$ because of higher particle mobility. Our prior study has extensively addressed the influence of changing $c$ on the thermodynamic properties.[43] In addition, an obvious bulge in $\kappa_T^*$ was observed near $T_g$, which may be attributed to small particles in the system, such as additives with short chain length or low cross-link density networks. A similar tendency has also been observed in our previous cross-linked thermosets without additives, especially the system with a low cross-link density such as $c = 0.04$ and $c = 0.23$.[43]

### 3.2. Segmental Relaxation Dynamics

The structural relaxation time $\tau_\alpha$ is a fundamental quantity that will be determined for the evaluation of basic dynamical properties. Specifically, $\tau_\alpha$ can be calculated by the self-part of the intermediate scattering function $F_s(q, t)$,

$$F_s(q, t) = \frac{1}{N}\langle \sum_{j=1}^{N} \exp\{ - i\mathbf{q}\cdot[\boldsymbol{r}_j(t) - \boldsymbol{r}_j(0)]\}\rangle \quad (4)$$

where $\boldsymbol{q}$ is the wave vector, $\boldsymbol{r}_j(t)$ represents the position of particle $j$ at time $t$, and $N$ is the total number of beads for both cross-linked polymer and additives. The wavenumber is selected as $q = |q| = 7.1$, a value closely approximating the location of the first peak in the static structure factor. The segmental relaxation time $\tau_\alpha$ is defined as the time when $F_s(q, t)$ decays to 0.2, consistent with the common definition in a wide range of polymeric glass formers.[44,56,57] In particular, in order to reduce errors in the estimation of $\tau_\alpha$, a time step of 0.002 or 0.01 is used in the high or low $T$, respectively.[44] As observed in various GF liquids,[12,58−60] $F_s(q, t)$ typically shows a two-step decay, which includes a "fast $\beta$-relaxation"[59,61] on the picosecond timescale and an $\alpha$-relaxation on a longer timescale, during which $F_s(q, t)$ gradually diminishes to zero, as shown in Figure S2 in the Supporting Information.

Figure 3a describes $\tau_\alpha$ as a function of $1/T$ for different $c$ and $m$. It is noted that $\tau_\alpha$ increases significantly with decreasing $T$ for the cross-linked polymer, similar to what has been observed for linear polymer melts with varying bending constraints and cohesive energy.[12,57] For fixed $m$, a higher cross-linked network shows a greater $\tau_\alpha$, which is consistent with some experimental findings for epoxy resins[31,32] and MD simulations for single-chain cross-linked nanoparticle melts.[62] As $c$ increases and $m$ decreases, there is a notable decrease in the segmental mobility. These trends align with expectations drawn from a wealth of experimental and simulation studies outlined in the Introduction and in our prior works,[37,43] and we next discuss these trends.

Figure 3a shows that the $T$-dependence of $\tau_\alpha$ obeys the Arrhenius regime at high temperatures and exhibits non-Arrhenius behavior at low temperatures, where the difference is related to the $c$ and $m$ of cross-linked thermosets. The Vogel−Fulcher−Tammann (VFT) relationship, $\tau_\alpha = \tau_0 \exp[DT_0/(T - T_0)]$, has successfully quantified the non-Arrhenius variation of $\tau_\alpha$ at low $T$ for a range of GF liquids,[18,20,62] where $\tau_0$ is a pre-exponential constant, the fitted values $T_0$ and $K \equiv 1/D$ are termed as the "VFT critical temperature" and the VFT-derived "kinetic fragility parameter", respectively (described in detail in Figure 4a,c).[13,57] As expected, the $\tau_\alpha$ data of our model thermosets with various $c$ and $m$ values follow the VFT relationship rather well (see Figure 3b).


https://doi.org/10.1021/acsengineeringau.3c00043
ACS Eng. Au 2023, 3, 512−526

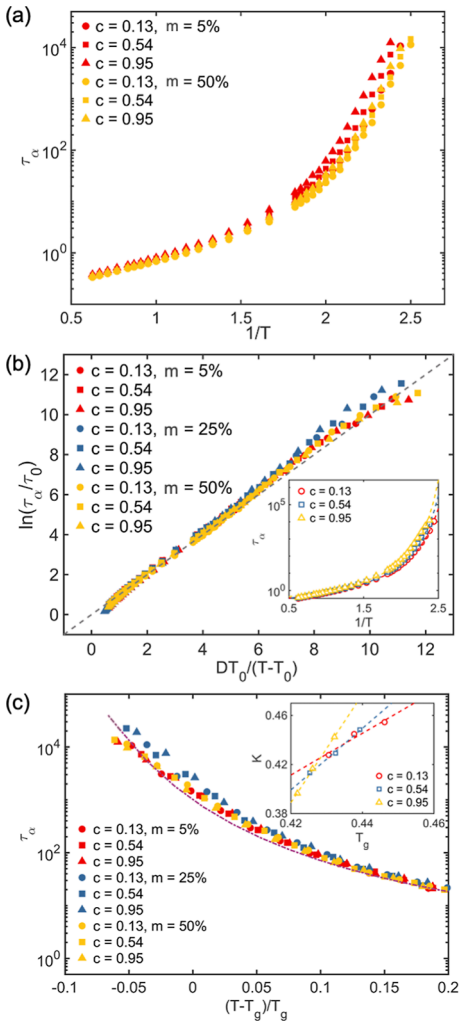


**Figure 3.** Temperature-dependent structural relaxation time $\tau_\alpha$. (a) $\tau_\alpha$ *vs* $1/T$ for different $c$ and $m$. $\tau_\alpha$ is determined by the time when $F_s(q, t)$ decays to 0.2. The difference of each simulation is relatively small in $\tau_\alpha$; hence, for the sake of clarity and conciseness, we have opted to omit the error bars. (b) VFT collapse of the $T$-dependence of $\tau_\alpha$. The dashed line indicates the VFT relation $\ln(\tau_\alpha/\tau_0) = DT/(T - T_0)$. The satisfactory alignment with the dashed line suggests that the Vogel–Fulcher–Tammann (VFT) equation effectively captures the relaxation dynamics across all cross-linked systems with differing values of $c$ and $m$. The inset shows the VFT fitting accuracy. (c) $\tau_\alpha$ as a function of $(T - T_g)/T_g$. The dashed line indicates the WLF fitting curve. Inset shows that $K$ is proportional to $T_g$. The inset shows $K$ as a function of $T_g$.

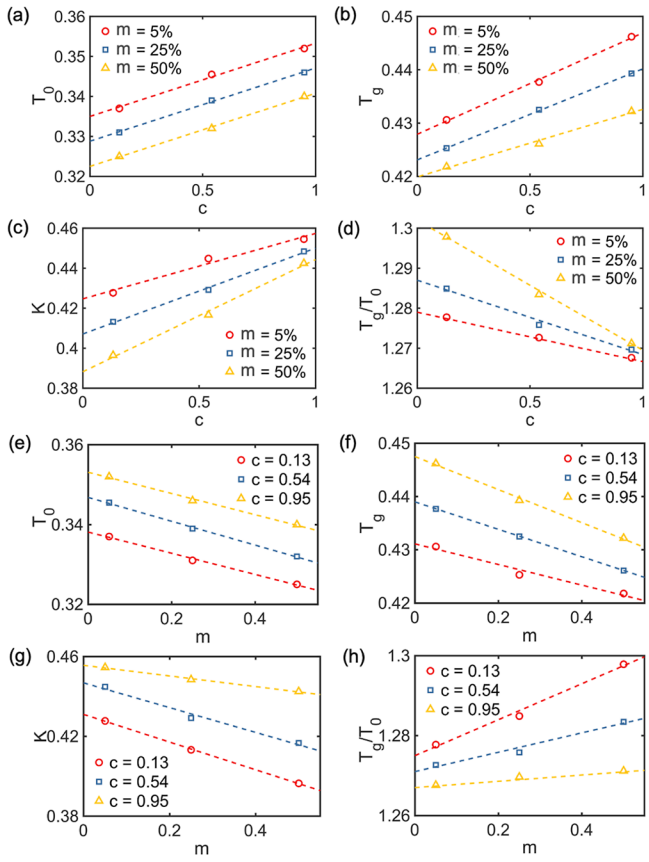


**Figure 4.** (a) VFT critical temperature $T_0$ as a function of $c$. (b) Glass transition temperature $T_g$ as a function of $c$. (c) Fragility parameter $K$ as a function of $c$. (d) $T_g/T_0$ as a function of $c$. (e) VFT critical temperature $T_0$ as a function of $m$. (f) Glass transition temperature $T_g$ as a function of $m$. (g) Fragility parameter $K$ as a function of $m$. (h) $T_g/T_0$ as a function of $m$.

Our previous work on the cross-linked polymers with varying $c$ indicated that the structural relaxation time can collapse onto a master curve when plotted against reduced temperature $(T - T_g)/T_g$ ($T_g$ will be described in a later section).[43] Here, we further explore the effect of additive mass percentage on the $\tau_\alpha$ at reduced temperature $(T - T_g)/T_g$ in the low-$T$ regime of glass formation ($T_g < T < 1.2\ T_g$). As shown in Figure 3c, the $\tau_\alpha$ data of cross-linked polymers with varying $c$ and $m$ collapse onto a master curve. This apparently near universal scaling relationship indicates that the cross-linked polymers with a range of $c$ and $m$ exhibit similar segmental relaxation dynamics at the same relative temperature distance from $T_g$, agreeing well with the empirical Williams–Landel–Ferry (WLF) equation.[63] A similar master curve of $\tau_\alpha$ at reduced temperature $T_g/T$ was also found based on a dynamic $T_g$ definition in a dense cross-linked polymer network with varying cross-link densities by Mei *et al.*, based on both experiments and CG-MD simulations, while there was no master curve observed when $T_g$ was defined from the variation of thermal expansion coefficient.[64] Based on the empirical WLF equation,[63] the relaxation time of various polymer materials is solely dependent on the temperature difference between $T$ and $T_g$, *i.e.*, $T - T_g$. Initially, it might appear paradoxical that the fragility parameter appears to have no bearing on comprehending the dynamics of glassy polymer materials based on this result alone. However, recent research by Dudowicz *et al.*[65] demonstrated that when $K$ and $T_g$ exhibit a proportional relationship, then the WLF scaling relationship with near universal constants $C_1$ and $C_2$ (eq 5) could be derived from the GET with constants specified. Interestingly, the inset of Figure 3c provides evidence that this proportionality relationship holds approximately. This interrelationship between fragility and $T_g$ simplifies the characterization of these materials' dynamics since the value of $T_g$ at the same time specifies the fragility in such materials. Guo and Simon[66] have recently tested six polymer materials to examine the universality of this reduced variable scaling, where the relationship was found to be widely applicable, but weakly dependent on pressure. We emphasize that the reduced variable scaling discussed here is not a typical feature of GF


https://doi.org/10.1021/acsengineeringau.3c00043
ACS Eng. Au 2023, 3, 512–526

liquids, including polymeric ones. It should be noted that the proportionality between $T_g$ and fragility is certainly not universal and the GET provides guidance on how to manipulate molecular parameters in such a way that fragility does not scale proportionately with $T_g$.[67]

This more general situation can be naturally characterized using a modified WLF equation (dashed line in Figure 3c)

$$\log[\tau_\alpha(T)/\tau_\alpha(T_g)] = -\frac{C_1^{(g)}(T - T_g)/T_g}{C_2^{(g)} + (T - T_g)/T_g} \quad (5)$$

where the modified WLF equation becomes formally equivalent to the VFT equation when $C_1^{(g)} = DT_0/[(T_g - T_0)\ln 10]$ and $C_2^{(g)} = (T_g - T_0)/T_g$. According to Dudowicz *et al.*,[65] $C_1^{(g)}$ describes the dynamical range of glass transition, and $1 - C_2^{(g)}$ provides a measure of the fragility associated with glass formation. $C_1^{(g)}$ and $1 - C_2^{(g)}$ are near "universal" constants in many GF materials,[65] but these parameters in the generalized WLF equation are variable fitting parameters in materials for which either $T_g$ is not proportional to fragility $K$ or for which the proportionality factor between $T_g$ and fragility has been significantly altered in comparison to the "typical" GF materials studied by WLF.[65] In the present simulated materials, $C_1^{(g)} = 3.66$ and $C_2^{(g)} = 0.21$ for all of the cross-linked thermosets considered.

As predicted by GET, the glass formation encompasses a broad transition having both thermodynamic and dynamic characteristics that must be characterized by multiple characteristic temperatures.[12,40,57,67] The effect of $c$ and $m$ on the characteristic temperatures and fragility of glass formation is next explored based on the VFT relation in order to better understand the dynamical properties of GF cross-linked thermosets with additives. Figure 4a shows the VFT critical temperature $T_0$ at which the structural relaxation time tends to become infinity, characterizing the termination of glass transition.[68,69] A nearly linear increase in $c$ is shown for cross-linked polymers with a broad $m$ range, and a similar linear relationship was also observed in our previous cross-linked polymers without additives.[43] It is notable that the progressive introduction of additives leads to an obvious decrease in $T_0$, well consistent with the faster relaxation dynamics of cross-linked thermosets with more additives exhibited in Figure 3a.

The glass transition temperature $T_g$ can be determined via the VFT equation for systems with different $c$ and $m$. According to the common experimental definition, $T_g$ is determined when the temperature at which the structural relaxation time becomes to 100 s, *i.e.*, $\tau_\alpha(T_g) = 100$ s.[3] However, limited by the cooling conditions and simulation techniques, it is difficult to reach equilibrium at low temperatures for a model of GF liquids.[43,60] In simulations of glass formation, a very narrow temperature range near $T_g$ is typically used to ensure accuracy.[12,18,57] To minimize the uncertainty in extrapolating to estimate $T_g$ *via* $\tau_\alpha$ data at significantly higher temperatures than experimental $T_g$, we calculate "computational" $T_g$ in this study. Specifically, we define $T_g$ as the temperature at which $\tau_\alpha(T_g) = 10^3$, corresponding to a laboratory timescale of approximately 1 ns, which is appropriate for the cooling rate employed in our simulations.[15,16,70] Although there exists a substantial difference in timescales between the computational and experimental measurements, previous works found a remarkable linear relationship between them.[43,60,71] A similar consistence was also observed in the form of cross-link density dependence of $T_g$ by Mei *et al.* using elastically collective nonlinear Langevin equation (ECNLE) theory, where $T_g$ was defined from different $\tau_\alpha$ timescales over nine decades.[64] Figure 4b shows that $T_g$ increases linearly with $c$, in agreement with the trend reported in a broad range of epoxy resins and networks polymers, where highly cross-linked thermosets usually exhibited a higher $T_g$.[39] In addition, $T_g$ decreases with an increase in $m$ for cross-linked systems with fixed $c$. As noted earlier, Dalle-Ferrier *et al.*[46] systematically investigated the influence of self-plasticizing additives on $T_g$ and fragility of polystyrene−oligomer mixtures, where the oligomer additives had the same chemical structure as polymer matrix. The experimental results indicated that the addition of oligomers resulted in a downward shift of $T_g$ and fragility for blends. The experiments performed by Ueberreiter and Kanig[45] for the polystyrene mixtures indicated that $T_g$ decreased with an increase in the number of end groups, and they suggested the now widely held belief that the end groups of polystyrene acted as "plasticizers", and thus led to "self-plasticization" of the polystyrene mixtures. In contrast, Riggleman *et al.*[39] found that the introduction of antiplasticizer additives led to a significant increase in $T_g$, while leading to a decrease of the fragility of glass formation at the same time when the additive was small and had a strong affinity for the polymer matrix. The affinity of the polymer additive can evidently have a large influence on the glassy dynamics and we plan to investigate this systematically in future work.

Various methods have been introduced to estimate the fragility parameter in glass formation studies, including the relative values of characteristic temperatures,[13,37,43] fragility parameter $K$,[13,37,43,62] and the conventional definition $m$.[23,32] Starr and Douglas[40] investigated the influence of NPs on fragility using different estimation techniques, and they found that fragility exhibited the same trend with increasing nanoparticle concentration. In this study, we use the VFT fragility parameter $K \equiv 1/D$ to avoid the uncertainty of estimating $T_g$ based on a narrow range of $\tau_\alpha$. A higher value of $K$ indicates a highly fragile GF system. We prefer this approach over using the "steepness parameter" $m_f$, which requires data near $T_g$, because of the limited $T$ range well above $T_g$ in the present work.[16,62] The fragility of cross-linked thermosets with a fixed mass percentage ($m$) increases with increasing cross-link density ($c$), consistent with trends observed in simulation works[37,43,62] and reported by Roland and Casalini.[28,72] for cross-linked poly(vinylethylene) networks using dielectric spectroscopy experiments. Figure 4c shows that fragility decreases as the mass percentage of additives increases over a wide range of $c$. A similar trend was also observed by Dalle-Ferrier *et al.*,[46] where the addition of polystyrene oligomers decreased the fragility of the polystyrene/oligomer blend while maintaining the same glassy properties as pure polystyrene. They also demonstrated that the change in fragility was associated with structural phenomena occurring at a scale significantly greater than that of the interchain or intermolecular separation. In addition, it has been demonstrated that the addition of oligomers,[46] plasticizers, and antiplasticizers[39,41,73] can decrease fragility compared to pure polymer melts.[47] According to the GET, fragility is primarily governed by packing efficiency at a molecular level, and polymers having more rigid backbones and fewer additives are usually more fragile.[23,67] However, the relationship between fragility and cross-link density is opposite to that between fragility and


https://doi.org/10.1021/acsengineeringau.3c00043
ACS Eng. Au 2023, 3, 512−526

additive mass percentage, making it more difficult to predict the relaxation in thermoset materials.

The characteristic temperature ratio $T_g/T_0$ provides a measure of the "breadth" of the glass transition, which is also found to be related to the fragility of glass formation. A smaller value of $T_g/T_0$ usually indicates a narrower temperature width of glass transition and thus a more "fragile" GF liquid. Figure 4d shows the effect of $m$ on the temperature width of the glass transition for the cross-linked polymers. The temperature width becomes smaller for systems with an elevated $c$ and a reduced $m$, where a competing effect of $c$ and $m$ on the temperature width of the glass transition is again observed. In addition, a higher $m$ of additives yields a stronger glass former, while a higher $c$ leads to a high fragility, consistent with the observation in Figure 4c. To further show the effect of mass percentage on the characteristic temperatures and fragility, here we have also put the characteristic temperatures/fragility as a function of mass percentage under different cross-link densities in Figure 4e–h.

In brief, the characteristic temperatures (*e.g.*, $T_g$ and $T_0$) and fragility of glass formation increase linearly with the cross-link density, while they exhibit a decreasing trend with an increasing additive mass percentage. An increase in the mass percentage of neutral polymer reduces the characteristic temperature and fragility of the system and correspondingly increases the plasticity, explaining the term "self-plasticizer". The competing effects of $c$ and additive $m$ on the characteristic temperatures and fragility of glass formation result in a more complicated prediction of the relaxation dynamics of GF cross-linked polymers.[12,69]

### 3.3. Molecular Mobility

To better understand how the mass percentage of additives influences the polymer dynamics, we next compute the Debye–Waller factor $\langle u^2 \rangle$, which is closely related to the local free volume of materials.[74] $\langle u^2 \rangle$ can be derived from X-ray and neutron scattering methods in experiments.[75,76] In MD simulations, $\langle u^2 \rangle$ can be calculated from the following equation

$$\langle r^2(t) \rangle = \frac{1}{N} \sum_{i=1}^{N} |r_i(t) - r_i(0)|^2 \quad (6)$$

where $r_i(t)$ is the coordinate of the $i$th monomer at time $t$, and $\langle r^2(t) \rangle$ is obtained from the average of all beads. $\langle u^2 \rangle$ is determined by the value of $\langle r^2(t) \rangle$ at a caging time of $t = 1$ for our model systems.

Considering the master curve of $\tau_\alpha$ observed at the reduced temperature $(T - T_g)/T_g$, Figure 5a estimates $\langle u^2 \rangle$ *vs* $T/T_g$ for different $c$ and additive $m$. The $\langle u^2 \rangle$ curves also collapse onto a master curve as a function of reduced temperature $T/T_g$ for cross-linked thermosets with a range of cross-link densities and additives mass percentages, consistent with the universal curve observed in the structural relaxation time in Figure 3c. The fit to $\langle u^2 \rangle$ highlights that $\langle u^2 \rangle$ exhibits greater sensitivity to changes of $T$ above $T_g$. In addition, the $\langle u^2 \rangle$ increases significantly with increasing $T$ for cross-linked thermosets due to the enhanced mobility of particles, as observed in linear polymer melts.[77] To better understand the influence of additives on the dynamical response of thermosets, $\langle u^2 \rangle$ is calculated as a function of $c$ for different components (*i.e.*, all beads, only network, and only additives, respectively). Figure 5b shows a clear conclusion that the $\langle u^2 \rangle$ decreases significantly with increasing $c$ for all specific beads of cross-linked thermosets, which further indicates that this is a system

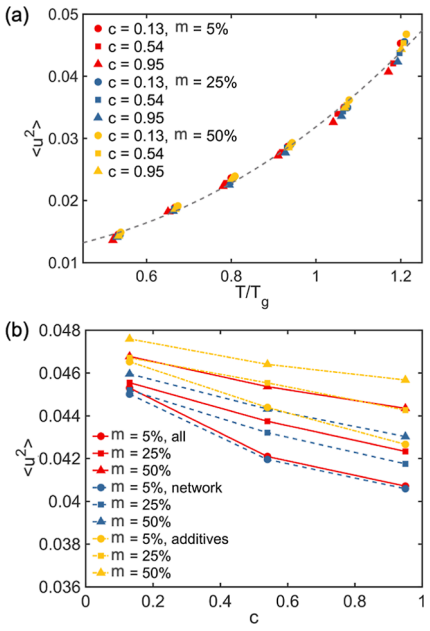


**Figure 5.** (a) Debye–Waller factor $\langle u^2 \rangle$ *vs* $T/T_g$ for different $c$ and $m$. (b) Debye–Waller factor $\langle u^2 \rangle$ *vs* $c$ for different beads $T = 0.45$.

of mutual influence. A similar phenomenon has also been observed in Diels–Alder-based thermo-reversibly cross-linked polymers,[78] where higher dynamics occurred in the polymers with a lower cross-link density. Based on the current settings of chain length and size, it is observed that additives have higher mobility than all beads and all beads have higher mobility than the network structure. This implies that additives can be considered to be accelerators of the system dynamics. Furthermore, this acceleration effect is more pronounced in highly cross-linked thermosets, as indicated by a wider range of mobility.

### 3.4. Mechanical Properties

Understanding the mechanical properties of cross-linked polymers is of vital importance to better improve and design their performance for a wide range of applications. Several basic mechanical properties are estimated for cross-linked polymers for different $c$ and $m$. The shear deformation is conducted at a fixed strain rate of $5 \times 10^{-4}$ 20 times for each condition. Figure 6a shows the shear simulation snapshots at different strains, where the gray squares describe the original simulation box. Figure 6b shows representative shear stress *vs* strain curves of cross-linked polymers with different $m$ at $T = 0.45$ and $c = 0.54$. The light-colored curves depict original stress values, and the colored solid curves show the averaged values. The shear modulus $G$ is determined by fitting stress–strain data in the linear regime. As the mass percentage becomes higher by modifying $m$ from 5% to 50%, the $G$ values and yield stress of the cross-linked thermosets are considerably reduced. Figure 6c shows the relationship between $G$ and $T$ at different mass percentages $m$ and cross-link densities $c$, where $G$ in its glassy state decreases significantly as the $T$ increases.[43,88] In addition, $G$ increases significantly with increasing $c$[37,43] and decreasing $m$ for cross-linked thermosets, where these two variables have a competing effect. The softening of cross-linked thermosets with the introduction of additives is reminiscent of the plasticization phenomenon.[84] The addition of small amounts of additives to a polymeric


https://doi.org/10.1021/acsengineeringau.3c00043
ACS Eng. Au 2023, 3, 512–526

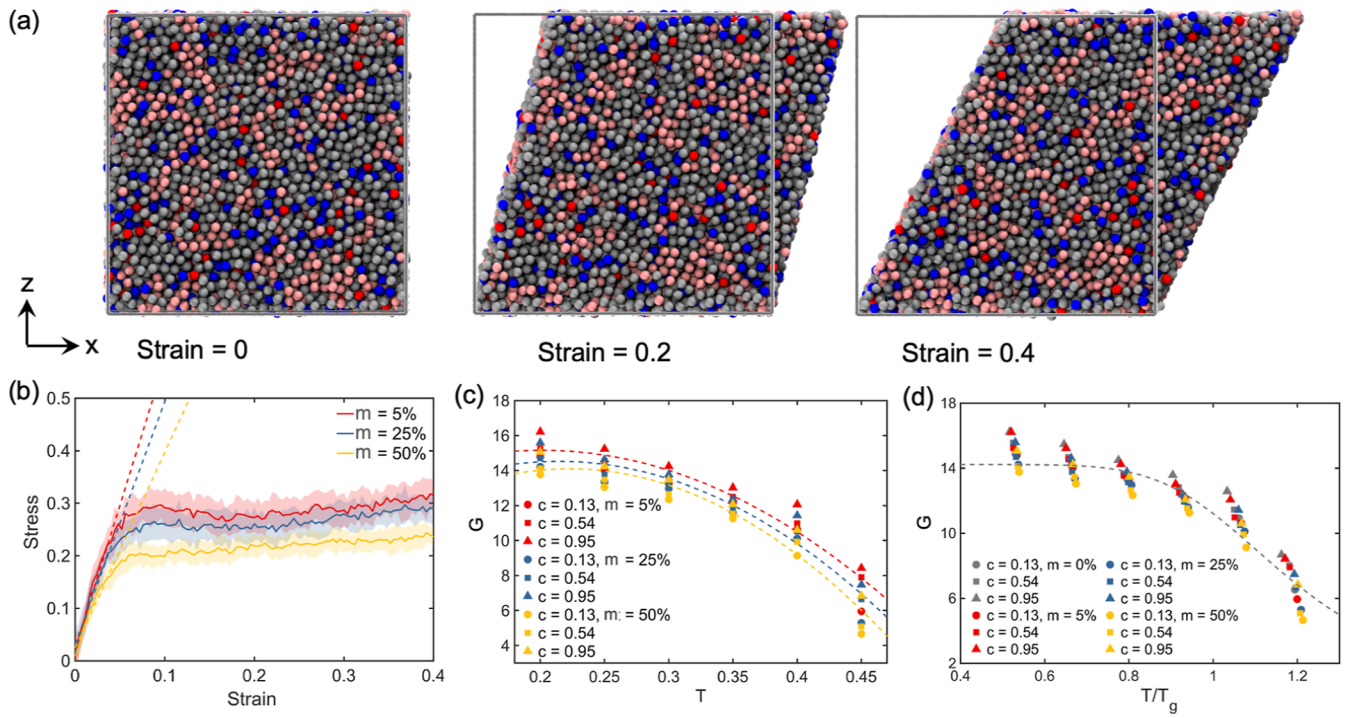


**Figure 6.** (a) Simulation snapshots of the thermosets under varying shear strains. (b) Shear stress *vs* strain curves at $T$ = 0.45 for cross-linked thermosets with different $m$ but a fixed $c$ = 0.54. (c) Shear modulus $G$ as a function of $T$. The dashed lines are fitting curves indicated by eq 7 for different mass percentages. (d) Shear modulus as a function of $T/T_g$. The fitting parameters ($G_0$, $\Delta_h$, and $\Delta_s$) are determined to be 14.2, −3.15, and −7.07. The dashed lines are fitting curves indicated by eq 7. Results for $m$ = 0% are only shown in this figure for the neat polymer reference case.

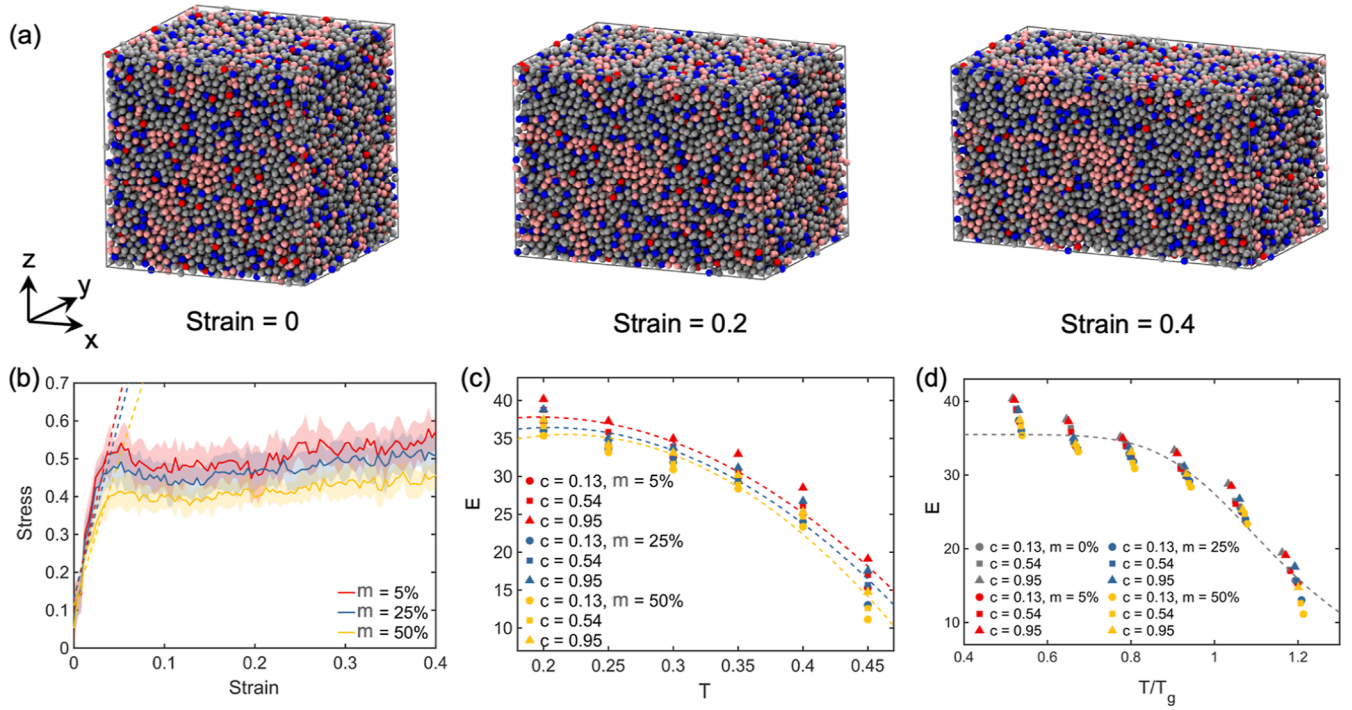


**Figure 7.** (a) Simulation snapshots of the thermosets at different tensile strains. (b) Tensile stress *vs* strain at $T$ = 0.45 for cross-linked thermosets with different mass percentages $m$ but a fixed cross-link density $c$ = 0.54. (c) Young's modulus $E$ *vs* $T$. The dashed lines are fitting curves for different $m$ values indicated by eq 7. (d) $E$ *vs* $T/T_g$. The fitting parameters ($B_0$, $\Delta_h$, and $\Delta_s$) are determined to be 103, −1.48, and −3.89. The dashed lines are fitting curves described in eq 7. Results for $m$ = 0% are only shown in this figure for the neat polymer reference case.

system usually leads to a depression of $T_g$ and a softening of polymeric materials.[79]

In our previous studies on the cross-linked polymers without additives,[37,43] we found that $G$ exhibited a universal scaling relationship with the reduced temperature $T/T_g$, and next, we investigate whether this reduced variable description remains applicable when different $m$ of additives are introduced. Remarkably, we find that $G$ indeed reduces to a master curve


https://doi.org/10.1021/acsengineeringau.3c00043
ACS Eng. Au 2023, 3, 512−526

when both $c$ and $m$ are varied (Figure 6d). To check the broadness of the applicability of the formula, we have added the results for $m$ = 0% (no additives, only networks), which show that this formula is also applicable to the cross-linked thermosets without additives. Similarly, Guo and Simon[29] found that the viscoelastic bulk moduli at $T_g$ were approximately constant for cross-linked polycyanurate networks for various $c$ using the dilatometer experiments under variable conditions.

Numerous networks arise through a self-assembly mechanism that entails thermally reversible binding of network chains. This procedure encompasses the autonomous organization of network fibers, subsequently resulting in branching and the formation of a network structure, potentially involving other molecules that govern this fiber branching phenomenon. In addressing this issue, Lin *et al.*[80] approached it in a comprehensive manner by employing streamlined models to elucidate the genesis of elasticity and self-assembly. They also derived a simplified "two-state" model that offers a practical and applicable approximation for a wide range of real-world scenarios, which we adopt as the basis for our analysis in this context. Having a simple and general parametric description of basic mechanical properties is crucial for material design and characterization. Such a description can facilitate the evaluation of these properties related to diverse molecular parameters, cross-link density, and temperature. A simple model expression for $G$ was derived by Lin *et al.*[80] through the application of lattice rigidity percolation theory, a two-state bond model, and others related to the development of a minimal model for glassy materials

$$\frac{G}{G_0} = \Phi,\ \Phi = 1/\{1 + \exp[(\Delta h - T\Delta s)/RT]\} \tag{7}$$

where the extent of self-assembly $\Phi$ is the basic order parameter governing self-assembly, the parameter $G_0$ represents the value of $G$ at low temperatures, while the empirical free energy parameters $\Delta h$ and $\Delta s$ describe the likelihood of the occurrence of stiff regions in the material, and $R$ is the fitting constant. Specifically, $G_0$, $\Delta h$, and $\Delta s$ are determined through curve fitting to the modulus data. The fitting constant, denoted as $R$ and termed the gas constant, remains constant with a fixed value of 1. The temperature-dependent behavior of moduli in glassy materials, such as polymers, biomaterials, and breakfast cereals,[80−82] has been described by a closely related phenomenological function termed the "Fermi function". This function has found wide applications in various studies. Lin *et al.*[80] demonstrated that the Fermi function could be deduced from an approximation of the model described by eq 7. We perceive this relationship for moduli in the glassy state as analogous to the empirical VFT equation used to correlate shear viscosity and diffusion for glass formers in the liquid state.

Similarly, the tensile deformation is conducted at the same fixed strain rate 20 times for each condition. The Young's modulus $E$ is determined from the linear portion of the average curves. Figure 7a indicates the snapshots at different tensile strains. Figure 7b shows the stress *vs* strain curves of cross-linked thermosets with additives at $T$ = 0.45 and $c$ = 0.54. The light-colored curves describe the range of original stress values, and the colored solid curves show the averaged values. Young's modulus $E$ is derived by fitting data of the linear regime. As the mass percentage increases from 5% to 50%, $E$ and yield stress of the cross-linked polymers gradually decrease. Figure 7c shows the relationship between $E$ and $T$ at different mass percentages $m$ and cross-link densities $c$. As observed in shear modulus $G$, $E$ in its simulated glassy state also decreases remarkably with increasing $T$. In addition, $E$ increases significantly with increasing $c$ and decreasing $m$ for cross-linked polymers, where these two variables have competing effects on $E$ to similar degrees. Moreover, Figure 7d shows that Young's modulus also reduces to a master curve when both $c$ and $m$ are varied, which shows a significant decreasing around $T_g$. The universal scaling relationship can be described using a similar semiempirical functional form indicated by eq 7, as that observed in shear modulus (Figure 6d) and in our previous studies.[37,43]

Given the practical importance of the bulk modulus $B$ in numerous structural applications, we carry out an examination of $c$ and $T$ dependence of this elastic property. The bulk modulus $B$ can be estimated simply from the isothermal compressibility $\kappa_T$. A significant decrease in $B$ as $T$ increases is observed in Figure 8a, as commonly reported in polymeric and metallic glass formers.[39,77,83] According our the findings, there is an increase in $B$ as the cross-link density increases, and the mass percentage of the additive decreases for cross-linked thermosets. The tendency about cross-linked density has been reported in our previous cross-linked thermosets system without additives.[37,43] It is worth noting that the impact of these two variables on $B$ is comparable in terms of magnitude. The modulus variation is tested at reduced temperature $T/T_g$, as shown in Figure 8b. The findings indicate that the bulk modulus exhibits a two-stage curve splitting around $T_g$ and can be fitted using a universal curve with a semiempirical functional

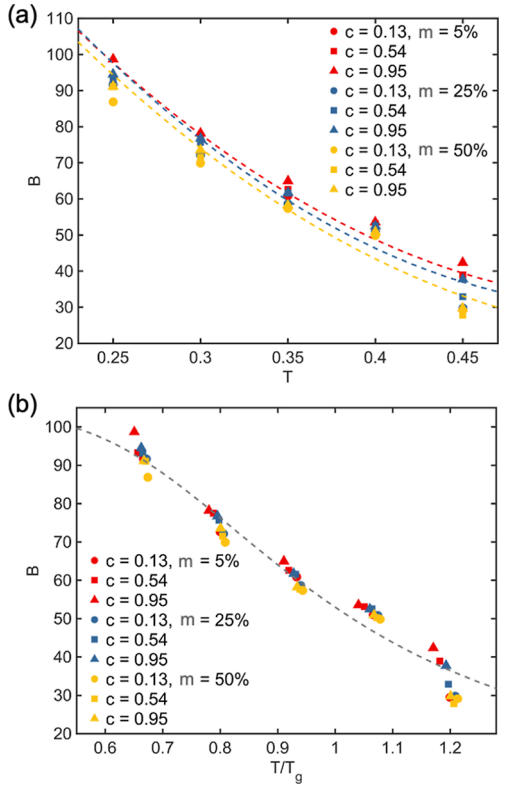


**Figure 8.** Estimation of bulk modulus for systems with varying $c$ and $m$. (a) Bulk modulus $B$ *vs* $T$. (b) $B$ *vs* $T/T_g$. The fitting parameters ($B_0$, $\Delta h$, and $\Delta s$) are determined to be 103.4664, −1.4798, and −3.8879. The dashed lines are fitting curves described in eq 7.


https://doi.org/10.1021/acsengineeringau.3c00043
ACS Eng. Au 2023, 3, 512−526

form indicated by eq 7, similar to the one presented in our prior works.[37,43] In summary, the universal curve observed in the different moduli ($G$, $E$, and $B$) at the reduced temperature emphasizes the critical role played by $T_g$ in the mechanical properties. In general, an increase in the mass percentage of neutral additives that acts as a self-plasticizer reduces the mechanical properties of the cross-linked system.

Recently, it has been acknowledged that the mechanical properties can be closely linked to molecular stiffness derived *via* $\langle u^2 \rangle$ for a broad range of glass formers.[77,84] Leporini and Puosi[85] previously constructed a master curve that related modulus and $\langle u^2 \rangle$, describing various glass formers with remarkable accuracy. In this study, we delve further into the relationship between the mechanical properties and $\langle u^2 \rangle$ with various $c$ and $m$. Consistent with prior studies,[37,43] we find that linear relationships between $G$ (or $E$) and local stiffness $k_BT/\langle u^2 \rangle$ generally hold for all the simulated systems (Figure 9a,b).

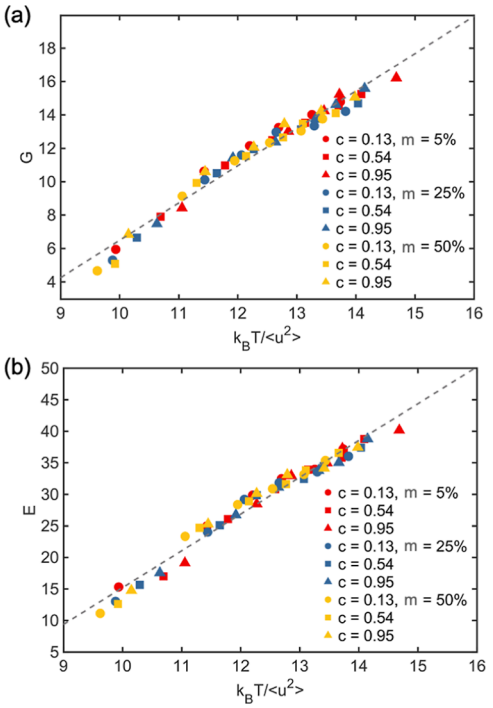


**Figure 9.** (a) $G$ *vs* $k_BT/\langle u^2 \rangle$ for systems with varying $c$ and $m$. The solid lines indicate the linear fitting. (b) $E$ *vs* $k_BT/\langle u^2 \rangle$ for systems with varying $c$ and $m$.

This aligns with the "universal relationship" discovered in fully flexible linear polymer melts[85] and Al−Sm[86] metallic glasses. Douglas and Xu[87] also reported a similar scaling relationship in simulations of linear polymer melts, indicating that this expression has some degree of universality over different materials. Xu *et al.*[88] utilized an approximate linear relation between $G_p$ and $k_BT/\langle u^2 \rangle$ in the GF polymer fluids having variable pressure, chain rigidity, chain length, and temperature. In the thermosets with additives, nearly all the data fall at the same linear relationship. However, our previous studies on the same networks but without additives[37,43] showed that different molecular parameter could influence the slope. Nevertheless, the underlying mechanism remains to be further explored. Considering the relationship between molecular stiffness and $\langle u^2 \rangle$, along with the customary interpretation of $\langle u^2 \rangle$ as an indicator, we regard $\langle u^2 \rangle$ as a measure for local material stiffness (as the definition of a local shear modulus at a molecular level is mathematically ambiguous).

### 3.5. Dynamical and Elastic Heterogeneity

It is widely acknowledged that the drop of the rate of relaxation dynamics upon cooling is linked to the emergence of dynamical heterogeneity in supercooled liquids. These heterogeneities are dynamical in nature, comprising domains of particles with varying mobility, which exist for a limited lifetime.[9,39,77] Such dynamical heterogeneity is a prominent feature of GF liquids, as well as thermoset polymers, as established in prior studies.[37,43] For example, Elder and co-workers[89] quantified this heterogeneity in cross-linked poly(dicyclopentadiene) networks using atomistic MD simulations, where chemically unique atom groups exhibited different root-mean-squared fluctuations, and atoms within linear segments had greater mobility compared to those in cross-links.[89] By analyzing molecular motion at different length scales, they also found that intrachain and interchain segmental motions were related to the $\alpha$-relaxation while localized motions were associated with sub-$T_g$ relaxations. As reported in our previous research on networks,[37,43] the incorporation of cross-links can lead to an increased heterogeneity in the distribution of local molecular stiffness in thermosets.

To better understand the influence of varying $m$ and $c$ on the dynamical heterogeneity of cross-linked polymers, the color maps of the local stiffness $1/\langle u^2 \rangle$ are plotted at a constant temperature $T$ = 0.45 (Figure 10). To facilitate a more intuitive comparison among plots, the color bar scale is kept consistent for all systems. Red regions in the color map correspond to domains where the particles exhibit very low amplitude motion, which indicates high local stiffness. Conversely, regions that appear in teal green indicate relatively soft regions with lower stiffness. Figure 10a shows the effect of the additive mass percentage on the dynamical heterogeneity, where increasing the additive mass percentage leads to a progressive enhancement in segmental mobility. When the additive mass percentage is relatively high ($m$ = 50%), and the temperature is fixed at $T$ = 0.45, which is higher than $T_g$. The particles show a reduced degree of heterogeneity and a smaller local stiffness. As a consequence, the color map is predominantly modified from red regions to teal blue regions (Figure 10a). As the additive concentration $m$ decreases, the cross-linked network becomes significantly stiffer and more heterogeneous. In Figure 10b, we observe that for systems with fixed $m$, the highly cross-linked network exhibits higher local stiffness and a greater level of heterogeneity, arising from the limited mobility imposed by the cross-links.[89] In addition, $m$ has a similar amplitude influence on the local stiffness compared to $c$. An increase in the mass percentage of neutral polymer that acts as a self-plasticizer increases the homogeneity of the system. It should be noted that in cross-linked polymers with additives, various factors beyond just the percentage of additives come into play. This encompasses intermolecular interactions, the stiffness of additive chains, chain length, and even the size of individual beads. These elements are crucial in influencing the relaxation, dynamics, and mechanical properties. Our forthcoming research endeavors will delve deeper into these intricate relationships.

## 4. CONCLUSIONS

By employing a bead−spring CG modeling approach, we systematically investigate the combined effects of cross-link


https://doi.org/10.1021/acsengineeringau.3c00043
ACS Eng. Au 2023, 3, 512−526

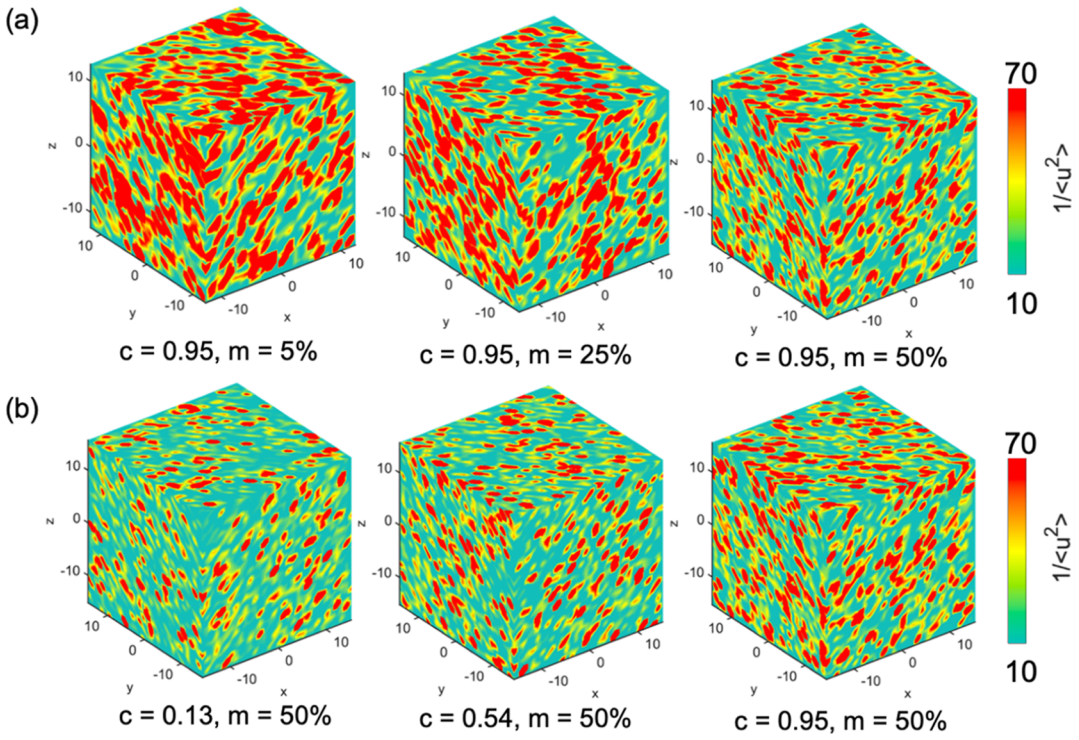


**Figure 10.** Color maps of local stiffness $1/\langle u^2 \rangle$ at constant temperature $T = 0.45$. (a) Effect of $m$. (b) Effect of $c$. Both the local stiffness and dynamical heterogeneity rise as $c$ increases and $m$ decreases.

density and additive mass percentage on the relaxation, dynamics, and mechanical properties of cross-linked polymers with additives. It is found that the additive mass percentage has a competing effect but with similar degrees on the relaxation dynamics compared to the cross-link density. It is notable that the characteristic temperatures (*i.e.*, the glass transition temperature $T_g$ and the VFT critical temperature $T_0$) and fragility of glass formation increase nearly linearly with increasing cross-link density, while they exhibit a decreasing trend with the increasing additive mass percentage. An increase in the mass percentage of the neutral polymer that acts as a self-plasticizer reduces the characteristic temperatures and fragility of the system and correspondingly increases the plasticity. Notably, apart from of the interplay between $m$ and $c$ on fragility, the structural relaxation time data of cross-linked thermosets, spanning a wide range of $c$ and $m$, can be described by a master curve when plotted against the reduced temperature $T/T_g$, as informed by the modified WLF function.

The assessment of mechanical properties (*i.e.*, $G$, $E$, and $B$) indicates that the additive mass percentage also has competing effects on the mechanical properties compared to varying cross-link density. An increase in the mass percentage of the neutral polymer that acts as a self-plasticizer reduces the mechanical properties of the system. Consistent with our recent studies, we observe a strong correlation between the Debye–Waller parameter $\langle u^2 \rangle$ and the mechanical properties of cross-linked polymers. The spatial distribution of local molecular stiffness $1/\langle u^2 \rangle$ is evaluated to explore the combined effect of cross-link density and additive mass percentage on the dynamical heterogeneity. Decreasing the additive mass percentage or increasing the cross-link density of cross-linked polymers can then lead to higher local molecular stiffness and an obviously increased level of dynamical heterogeneity. This study offers valuable insights into the fundamental impact of additive mass percentage and cross-link density on the relaxation dynamics and mechanical properties of GF cross-linked thermosets. These findings should prove beneficial in the development of structure–property relationships for this class of materials, as well as for other related network materials. By identifying the key variables that affect the material's properties, this work provides a starting point for optimizing the properties of GF cross-linked thermosets for various applications. Additionally, the results presented here may help guide future research into the design and synthesis of new materials with tailored mechanical and relaxation properties.

## ■ ASSOCIATED CONTENT

### Supporting Information

The Supporting Information is available free of charge at https://pubs.acs.org/doi/10.1021/acsengineeringau.3c00043.

Basic thermodynamic properties; self-part of the intermediate scattering function; glass transition temperature; volumetric cross-link density; 2D color maps of particle distribution; 2D color maps of local stiffness; and cross-link density *vs* iterations; and mechanical properties with error bar (PDF)

## ■ AUTHOR INFORMATION

### Corresponding Authors

**Jack F. Douglas** − *Materials Science and Engineering Division, National Institute of Standards and Technology, Gaithersburg, Maryland 20899, United States;* orcid.org/0000-0001-7290-2300; Email: jack.douglas@nist.gov

**Wenjie Xia** − *Department of Aerospace Engineering, Iowa State University, Ames, Iowa 50011, United States;* orcid.org/0000-0001-7870-0128; Email: wxia@iastate.edu



https://doi.org/10.1021/acsengineeringau.3c00043
*ACS Eng. Au* 2023, 3, 512−526

## Author

**Wenjian Nie** − *Department of Civil, Construction and Environmental Engineering, North Dakota State University, Fargo, North Dakota 58108, United States*

Complete contact information is available at: https://pubs.acs.org/10.1021/acsengineeringau.3c00043


## Author Contributions

CRediT: **Wenjian Nie** data curation, formal analysis, software, writing-original draft; **Jack F. Douglas** investigation, supervision, validation, writing-review & editing; **Wenjie Xia** conceptualization, funding acquisition, investigation, methodology, project administration, resources, supervision, writing-review & editing.

## Notes

The authors declare no competing financial interest.

## ■ ACKNOWLEDGMENTS

The authors acknowledge the support from the U.S. Office of Naval Research (award no. N00014-22-1-2129). J.D.F. acknowledges the support from the National Institutes of Standards and Technology.

## ■ REFERENCES


(1) Hayashi, M. Implantation of Recyclability and Healability into Cross-Linked Commercial Polymers by Applying the Vitrimer Concept. *Polymers* **2020**, *12*, 1322 MDPI: AG.

(2) Tang, Y.; Xu, W.; Niu, S.; Zhang, Z.; Zhang, Y.; Jiang, Z. Crosslinked Dielectric Materials for High-Temperature Capacitive Energy Storage. *J. Mater. Chem. A* **2021**, *9*, 10000−10011 Royal Society of Chemistry.

(3) Napolitano, S.; Glynos, E.; Tito, N. B. Glass Transition of Polymers in Bulk, Confined Geometries, and near Interfaces. *Rep. Prog. Phys.* **2017**, *80*, 036602 Institute of Physics Publishing.

(4) Temelkuran, B.; Hart, S. D.; Benoit, G.; Joannopoulos, J. D.; Fink, Y. Wavelength-Scalable Hollow Optical Fibres with Large Photonic Bandgaps for CO2 Laser Transmission. *Nature* **2002**, *420* (6916), 650−653.

(5) Casalini, R.; Corezzi, S.; Fioretto, D.; Livi, A.; Rolla, P. A. Unified Dielectric Description of the Dynamics of Polymeric Systems Undergoing Either Thermal or Chemical Vitrification. *Chem. Phys. Lett.* **1996**, *258*, 470−476.

(6) Sauvant, V.; Halary, J. L. Improvement of the Performance of Epoxy-Amine Thermosets by Antiplasticizer-Induced Nano-Scale Phase Separation during Cure. *Compos. Sci. Technol.* **2002**, *62* (4), 481−486.

(7) Rana, D.; Sauvant, V.; Halary, J. L. Molecular Analysis of Yielding in Pure and Antiplasticized Epoxy-Amine Thermosets. *J. Mater. Sci.* **2002**, *37* (24), 5267−5274.

(8) Morel, E.; Bellenger, V.; Bocquet, M.; Verdu, J. Structure-Properties Relationships for Densely Cross-Linked Epoxide-Amine Systems Based on Epoxide or Amine Mixtures Part 3 Elastic Properties. *J. Mater. Sci.* **1989**, *24*, 69−75.

(9) Elder, R. M.; Long, T. R.; Bain, E. D.; Lenhart, J. L.; Sirk, T. W. Mechanics and Nanovoid Nucleation Dynamics: Effects of Polar Functionality in Glassy Polymer Networks. *Soft Matter* **2018**, *14* (44), 8895−8911.

(10) Lee, A.; Mckenna, G. B. Effect of Crosslink Density on Physical Ageing of Epoxy Networks. *Polymer* **1988**, *29*, 1812−1817.

(11) Kannurpatti, A. R.; Bowman, C. N. Structural Evolution of Dimethacrylate Networks Studied by Dielectric Spectroscopy. *Macromolecules* **1998**, *31*, 3311−3316.

(12) Xu, W. S.; Douglas, J. F.; Xu, X. Role of Cohesive Energy in Glass Formation of Polymers with and without Bending Constraints. *Macromolecules* **2020**, *53* (22), 9678−9697.

(13) Xu, W. S.; Douglas, J. F.; Xu, X. Molecular Dynamics Study of Glass Formation in Polymer Melts with Varying Chain Stiffness. *Macromolecules* **2020**, *53* (12), 4796−4809.

(14) Huang, J. H.; Sun, D. D.; Lu, R. X. Glass Transition and Dynamics of Semiflexible Polymer Brushes. *Phys. Chem. Chem. Phys.* **2021**, *23* (25), 13895−13904.

(15) Zhang, W.; Douglas, J. F.; Chremos, A.; Starr, F. W. Structure and Dynamics of Star Polymer Films from Coarse-Grained Molecular Simulations. *Macromolecules* **2021**, *54* (12), 5344−5353.

(16) Xia, W.; Song, J.; Hsu, D. D.; Keten, S. Side-Group Size Effects on Interfaces and Glass Formation in Supported Polymer Thin Films. *J. Chem. Phys.* **2017**, *146* (20), 203311.

(17) Fan, J.; Emamy, H.; Chremos, A.; Douglas, J. F.; Starr, F. W. Dynamic Heterogeneity and Collective Motion in Star Polymer Melts. *J. Chem. Phys.* **2020**, *152* (5), 054904.

(18) Vargas-Lara, F.; Pazmiño Betancourt, B. A.; Douglas, J. F. Influence of Knot Complexity on Glass-Formation in Low Molecular Mass Ring Polymer Melts. *J. Chem. Phys.* **2019**, *150* (10), 101103.

(19) Xu, W. S.; Douglas, J. F.; Freed, K. F. Influence of Pressure on Glass Formation in a Simulated Polymer Melt. *Macromolecules* **2017**, *50* (6), 2585−2598.

(20) Duarte, D. M.; Tu, W.; Dzienia, A.; Adrjanowicz, K. Study on the Effect of Side-Chain Group on the Segmental Dynamics of Selected Methacrylate Polymers at Ambient and High Pressures. *Polymer* **2019**, *183*, 121860.

(21) Higuchi, C.; Horvath, D.; Marcou, G.; Yoshizawa, K.; Varnek, A. Prediction of the Glass-Transition Temperatures of Linear Homo/Heteropolymers and Cross-Linked Epoxy Resins. *ACS Appl. Polym. Mater.* **2019**, *1* (6), 1430−1442.

(22) Xie, R.; Weisen, A. R.; Lee, Y.; Aplan, M. A.; Fenton, A. M.; Masucci, A. E.; Kempe, F.; Sommer, M.; Pester, C. W.; Colby, R. H.; Gomez, E. D. Glass Transition Temperature from the Chemical Structure of Conjugated Polymers. *Nat. Commun.* **2020**, *11* (1), 893.

(23) Kunal, K.; Robertson, C. G.; Pawlus, S.; Hahn, S. F.; Sokolov, A. P. Role of Chemical Structure in Fragility of Polymers: A Qualitative Picture. *Macromolecules* **2008**, *41* (19), 7232−7238.

(24) Wang, C.-Y.; Ediger, M. D. Spatially Heterogeneous Dynamics in Thermoset Resins Below the Glass-Transition Temperature: Effect of Temperature and Composition. *J. Polym. Sci., Part B: Polym. Phys.* **2000**, *38*, 2232−2239.

(25) Inoue, R.; Kanaya, T.; Nishida, K.; Tsukushi, I.; Taylor, J.; Levett, S.; Gabrys, B. J. Dynamic Anisotropy and Heterogeneity of Polystyrene Thin Films as Studied by Inelastic Neutron Scattering. *Eur. Phys. J. E* **2007**, *24* (1), 55−60.

(26) Liu, Y. H.; Wang, D.; Nakajima, K.; Zhang, W.; Hirata, A.; Nishi, T.; Inoue, A.; Chen, M. W. Characterization of Nanoscale Mechanical Heterogeneity in a Metallic Glass by Dynamic Force Microscopy. *Phys. Rev. Lett.* **2011**, *106* (12), 125504.

(27) Lossada, F.; Abbasoglu, T.; Jiao, D.; Hoenders, D.; Walther, A. Glass Transition Temperature Regulates Mechanical Performance in Nacre-Mimetic Nanocomposites. *Macromol. Rapid Commun.* **2020**, *41* (20), 2000380.

(28) Casalini, R.; Roland, C. M. Effect of Crosslinking on the Secondary Relaxation in Polyvinylethylene. *J. Polym. Sci., Part B: Polym. Phys.* **2010**, *48* (5), 582−587.

(29) Guo, J.; Simon, S. L. Effect of Crosslink Density on the Pressure Relaxation Response of Polycyanurate Networks. *J. Polym. Sci., Part B: Polym. Phys.* **2009**, *47* (24), 2477−2486.

(30) Sasaki, T.; Uchida, T.; Sakurai, K. Effect of Crosslink on the Characteristic Length of Glass Transition of Network Polymers. *J. Polym. Sci., Part B: Polym. Phys.* **2006**, *44* (14), 1958−1966.

(31) Beiner, M.; Ngai, K. L. Interrelation between Primary and Secondary Relaxations in Polymerizing Systems Based on Epoxy Resins. *Macromolecules* **2005**, *38* (16), 7033−7042.

(32) Alves, N. M.; Gómez Ribelles, J.; Mano, J. F. Enthalpy Relaxation Studies in Polymethyl Methacrylate Networks with Different Crosslinking Degrees. *Polymer* **2005**, *46* (2), 491−504.

(33) Bronnikov, S.; Kostromin, S.; Asandulesa, M.; Podshivalov, A.; Timpu, D. Morphology, Structure, and Segmental Dynamics in

Polyazomethine/Hybrid Carbon Nanofillers Composites. *Polym. Compos.* **2019**, *40* (12), 4638−4649.
(34) Reza-E-Rabby, M.; Jeelani, S.; Rangari, V. K. Structural Analysis of Polyhedral Oligomeric Silsesquioxane Coated Sic Nanoparticles and Their Applications in Thermoset Polymers. *J. Nanomater.* **2015**, *2015*, 1−13.
(35) Hernández, E.; Mendoza Zelis, P.; Bruvera, I.; Mosiewicki, M. A.; Marcovich, N. E. Magnetic Nanocomposites Based on Thermoset Polymers with Outstanding Amount of Green Carbon. *J. Polym. Environ.* **2023**, *31* (1), 149−161.
(36) Yang, Z.; Xu, X.; Douglas, J. F.; Xu, W. Molecular Dynamics Investigation of the Pressure Dependence of Glass Formation in a Charged Polymer Melt. *Macromolecules* **2023**, *56*, 4049−4064.
(37) Zheng, X.; Guo, Y.; Douglas, J. F.; Xia, W. Competing Effects of Cohesive Energy and Cross-Link Density on the Segmental Dynamics and Mechanical Properties of Cross-Linked Polymers. *Macromolecules* **2022**, *55*, 9990−10004.
(38) Spyridakou, M.; Iliopoulou, E.; Peponaki, K.; Alexandris, S.; Filippidi, E.; Floudas, G. Heterogeneous Local Dynamics in Mussel-Inspired Elastomers. *Macromolecules* **2023**, *56*, 4336−4345.
(39) Riggleman, R. A.; Douglas, J. F.; De Pablo, J. J. Antiplasticization and the Elastic Properties of Glass-Forming Polymer Liquids. *Soft Matter* **2010**, *6* (2), 292−304.
(40) Starr, F. W.; Douglas, J. F. Modifying Fragility and Collective Motion in Polymer Melts with Nanoparticles. *Phys. Rev. Lett.* **2011**, *106* (11), 115702.
(41) Stukalin, E. B.; Douglas, J. F.; Freed, K. F. Plasticization and Antiplasticization of Polymer Melts Diluted by Low Molar Mass Species. *J. Chem. Phys.* **2010**, *132* (8), 084504.
(42) Mangalara, J. H.; Simmons, D. S. Tuning Polymer Glass Formation Behavior and Mechanical Properties with Oligomeric Diluents of Varying Stiffness. *ACS Macro Lett.* **2015**, *4* (10), 1134−1138.
(43) Zheng, X.; Guo, Y.; Douglas, J. F.; Xia, W. Understanding the Role of Cross-Link Density in the Segmental Dynamics and Elastic Properties of Cross-Linked Thermosets. *J. Chem. Phys.* **2022**, *157* (6), 064901.
(44) Pan, D.; Sun, Z. Y. Influence of Chain Stiffness on the Dynamical Heterogeneity and Fragility of Polymer Melts. *J. Chem. Phys.* **2018**, *149* (23), 234904.
(45) Ueberreiter, K.; Kanig, G. Self-Plasticization of Polymers. *J. Colloid Sci.* **1952**, *7* (6), 569−583.
(46) Dalle-Ferrier, C.; Simon, S.; Zheng, W.; Badrinarayanan, P.; Fennell, T.; Frick, B.; Zanotti, J. M.; Alba-Simionesco, C. Consequence of Excess Configurational Entropy on Fragility: The Case of a Polymer-Oligomer Blend. *Phys. Rev. Lett.* **2009**, *103* (18), 185702.
(47) Dimarzio, E. A.; Gibbs, J. H. Molecular Interpretation of Glass Temperature Depression by Plasticizers. *J. Polym. Sci., Part A: Gen. Pap.* **1963**, *1* (4), 1417−1428.
(48) Kremer, K.; Grest, G. S. Dynamics of Entangled Linear Polymer Melts: A Molecular-Dynamics Simulation. *J. Chem. Phys.* **1990**, *92* (8), 5057−5086.
(49) Thompson, A. P.; Aktulga, H. M.; Berger, R.; Bolintineanu, D. S.; Brown, W. M.; Crozier, P. S.; in 't Veld, P. J.; Kohlmeyer, A.; Moore, S. G.; Nguyen, T. D.; Shan, R.; Stevens, M. J.; Tranchida, J.; Trott, C.; Plimpton, S. J. LAMMPS - a Flexible Simulation Tool for Particle-Based Materials Modeling at the Atomic, Meso, and Continuum Scales. *Comput. Phys. Commun.* **2022**, *271*, 108171.
(50) Varshney, V.; Patnaik, S. S.; Roy, A. K.; Farmer, B. L. A Molecular Dynamics Study of Epoxy-Based Networks: Cross-Linking Procedure and Prediction of Molecular and Material Properties. *Macromolecules* **2008**, *41* (18), 6837−6842.
(51) Shokuhfar, A.; Arab, B. The Effect of Cross Linking Density on the Mechanical Properties and Structure of the Epoxy Polymers: Molecular Dynamics Simulation. *J. Mol. Model.* **2013**, *19* (9), 3719−3731.
(52) Bandyopadhyay, A.; Valavala, P. K.; Clancy, T. C.; Wise, K. E.; Odegard, G. M. Molecular Modeling of Crosslinked Epoxy Polymers: The Effect of Crosslink Density on Thermomechanical Properties. *Polymer* **2011**, *52* (11), 2445−2452.
(53) Simon, S. L.; Mckenna, G. B.; Sindt, O. Modeling the Evolution of the Dynamic Mechanical Properties of a Commercial Epoxy during Cure after Gelation. *J. Appl. Polym. Sci.* **2000**, *76* (4), 495−508.
(54) Gupta, V. B.; Brahatheeswaran, C. Molecular Packing and Free Volume in Crosslinked Epoxy Networks. *Polymer* **1991**, *32* (10), 1875−1884.
(55) Gupta, V. B.; Drzal, L. T.; Lee, C. Y.-C.; Rich, M. J. The Temperature-dependence of Some Mechanical Properties of a Cured Epoxy Resin System. *Polym. Eng. Sci.* **1985**, *25* (13), 812−823.
(56) Xu, W. S.; Douglas, J. F.; Freed, K. F. Influence of Cohesive Energy on the Thermodynamic Properties of a Model Glass-Forming Polymer Melt. *Macromolecules* **2016**, *49* (21), 8341−8354.
(57) Xu, W. S.; Douglas, J. F.; Freed, K. F. Influence of Cohesive Energy on Relaxation in a Model Glass-Forming Polymer Melt. *Macromolecules* **2016**, *49* (21), 8355−8370.
(58) Wu, J. B.; Li, S. J.; Liu, H.; Qian, H. J.; Lu, Z. Y. Dynamics and Reaction Kinetics of Coarse-Grained Bulk Vitrimers: A Molecular Dynamics Study. *Phys. Chem. Chem. Phys.* **2019**, *21* (24), 13258−13267.
(59) Giuntoli, A.; Puosi, F.; Leporini, D.; Starr, F. W.; Douglas, J. F. Predictive relation for the $\alpha$-relaxation time of a coarse-grained polymer melt under steady shear. *Sci. Adv.* **2020**, *6* (17), 1−10.
(60) Zhang, H.; Wang, X.; Yu, H. B.; Douglas, J. F. Dynamic heterogeneity, cooperative motion, and Johari−Goldstein $\beta$-relaxation in a metallic glass-forming material exhibiting a fragile-to-strong transition. *Eur. Phys. J. E* **2021**, *44* (4), 56.
(61) Pazmiño Betancourt, B. A.; Starr, F. W.; Douglas, J. F. String-like Collective Motion in the $\alpha$- and $\beta$-Relaxation of a Coarse-Grained Polymer Melt. *J. Chem. Phys.* **2018**, *148* (10), 104508.
(62) Jia, X. M.; Lin, W. F.; Zhao, H. Y.; Qian, H. J.; Lu, Z. Y. Supercooled Melt Structure and Dynamics of Single-Chain Nanoparticles: A Computer Simulation Study. *J. Chem. Phys.* **2021**, *155* (5), 054901.
(63) Williams, M. L.; Landel, R. F.; Ferry, J. D. The Temperature Dependence of Relaxation Mechanisms in Amorphous Polymers and Other Glass-Forming Liquids. *J. Am. Chem. Soc.* **1955**, *77*, 3701−3707.
(64) Mei, B.; Lin, T. W.; Sheridan, G. S.; Evans, C. M.; Sing, C. E.; Schweizer, K. S. Structural Relaxation and Vitrification in Dense Cross-Linked Polymer Networks: Simulation, Theory, and Experiment. *Macromolecules* **2022**, *55*, 4159−4173.
(65) Dudowicz, J.; Douglas, J. F.; Freed, K. F. The Meaning of the "Universal" WLF Parameters of Glass-Forming Polymer Liquids. *J. Chem. Phys.* **2015**, *142* (1), 014905.
(66) Guo, J.; Simon, S. L. Thermodynamic Scaling of Polymer Dynamics versus T - Tg Scaling. *J. Chem. Phys.* **2011**, *135* (7), 074901.
(67) Stukalin, E. B.; Douglas, J. F.; Freed, K. F. Application of the entropy theory of glass formation to poly($\alpha$-olefins). *J. Chem. Phys.* **2009**, *131* (11), 1−13.
(68) Xu, W. S.; Douglas, J. F.; Sun, Z. Y. Polymer Glass Formation: Role of Activation Free Energy, Configurational Entropy, and Collective Motion. *Macromolecules* **2021**, *54* (7), 3001−3033.
(69) Dudowicz, J.; Freed, K. F.; Douglas, J. F. Generalized Entropy Theory of Polymer Glass Formation. *Adv. Chem. Phys.* **2007**, *137*, 125−222.
(70) Mangalara, J. H.; Marvin, M. D.; Wiener, N. R.; Mackura, M. E.; Simmons, D. S. Does Fragility of Glass Formation Determine the Strength of Tg-Nanoconfinement Effects? *J. Chem. Phys.* **2017**, *146* (10), 104902.
(71) Pinski, F. P.; Peter, C. P.; Valeev, C. R.; Neese, F. SparseMaps - A Systematic Infrastructure for Reduced Scaling Electronic Structure Methods. V. Linear Scaling Explicitly Correlated Coupled-Cluster Method with Pair Natural Orbitals. *J. Chem. Phys.* **2017**, *146* (17), 174108.


https://doi.org/10.1021/acsengineeringau.3c00043
*ACS Eng. Au* 2023, 3, 512−526

(72) Roland, C. M. Constraints on Local Segmental Motion in Poly(Vinylethylene) Networks. *Macromolecules* **1994**, *27* (15), 4242−4247.
(73) Riggleman, R. A.; Douglas, J. F.; De Pablo, J. J. Tuning Polymer Melt Fragility with Antiplasticizer Additives. *J. Chem. Phys.* **2007**, *126* (23), 234903.
(74) Pazmiño Betancourt, B. A.; Hanakata, P. Z.; Starr, F. W.; Douglas, J. F. Quantitative Relations between Cooperative Motion, Emergent Elasticity, and Free Volume in Model Glass-Forming Polymer Materials. *Proc. Natl. Acad. Sci. U.S.A.* **2015**, *112* (10), 2966−2971.
(75) Griffin, A.; Jobic, H. Theory of the Effective Debye-Waller Factor in Neutron Scattering from High Frequency Molecular Modes. *J. Chem. Phys.* **1981**, *75* (12), 5940−5943.
(76) Bellissent-Funel, M. C.; Filabozzi, A.; Chen, S. H. Measurement of Coherent Debye-Waller Factor in in Vivo Deuterated C-Phycocyanin by Inelastic Neutron Scattering. *Biophys. J.* **1997**, *72* (4), 1792−1799.
(77) Alesadi, A.; Xia, W. Understanding the Role of Cohesive Interaction in Mechanical Behavior of a Glassy Polymer. *Macromolecules* **2020**, *53* (7), 2754−2763.
(78) Orozco, F.; Li, J.; Ezekiel, U.; Niyazov, Z.; Floyd, L.; Lima, G. M. R.; Winkelman, J. G. M.; Moreno-Villoslada, I.; Picchioni, F.; Bose, R. K. Diels-Alder-Based Thermo-Reversibly Crosslinked Polymers: Interplay of Crosslinking Density, Network Mobility, Kinetics and Stereoisomerism. *Eur. Polym. J.* **2020**, *135*, 109882.
(79) Ferry, J. D. *Viscoelastic Properties of Polymers*; 3rd Ed.; Wiley: New York, 1980; p 672.
(80) Lin, D. C.; Douglas, J. F.; Horkay, F. Development of Minimal Models of the Elastic Properties of Flexible and Stiff Polymer Networks with Permanent and Thermoreversible Cross-Links. *Soft Matter* **2010**, *6* (15), 3548−3561.
(81) Peleg, M. Mapping the Stiffness-Temperature-Moisture Relationship of Solid Biomaterials at and around Their Glass Transition. *Rheol. Acta* **1993**, *32* (6), 575−580.
(82) Nakanishi, S.; Yoshikawa, H.; Shoji, S.; Sekkat, Z.; Kawata, S. Size Dependence of Transition Temperature in Polymer Nanowires. *J. Phys. Chem. B* **2008**, *112* (12), 3586−3589.
(83) Wang, X.; Zhang, H.; Douglas, J. F. The Initiation of Shear Band Formation in Deformed Metallic Glasses from Soft Localized Domains. *J. Chem. Phys.* **2021**, *155* (20), 204504.
(84) Xia, W.; Song, J.; Jeong, C.; Hsu, D. D.; Phelan, F. R.; Douglas, J. F.; Keten, S. Energy-Renormalization for Achieving Temperature Transferable Coarse-Graining of Polymer Dynamics. *Macromolecules* **2017**, *50* (21), 8787−8796.
(85) Puosi, F.; Leporini, D. The Kinetic Fragility of Liquids as Manifestation of the Elastic Softening. *Eur. Phys. J. E* **2015**, *38* (8), 87.
(86) Zhang, H.; Wang, X.; Yu, H. B.; Douglas, J. F. Fast Dynamics in a Model Metallic Glass-Forming Material. *J. Chem. Phys.* **2021**, *154* (8), 084505.
(87) Douglas, J. F.; Xu, W. S. Equation of State and Entropy Theory Approach to Thermodynamic Scaling in Polymeric Glass-Forming Liquids. *Macromolecules* **2021**, *54* (7), 3247−3269.
(88) Xu, X.; Douglas, J. F.; Xu, W.-S. Parallel Emergence of Rigidity and Collective Motion in a Family of Simulated Glass-Forming Polymer Fluids. *Macromolecules* **2023**, *56*, 4929−4951.
(89) Elder, R. M.; Andzelm, J. W.; Sirk, T. W. A Molecular Simulation Study of the Glass Transition of Cross-Linked Poly-(Dicyclopentadiene) Networks. *Chem. Phys. Lett.* **2015**, *637*, 103−109.


https://doi.org/10.1021/acsengineeringau.3c00043
*ACS Eng. Au* 2023, 3, 512−526